Robust elements of Snowball Earth atmospheric circulation and oases for life

Dorian S. Abbot, Aiko Voigt, Dawei Li, Guillaume Le Hir, Raymond T. Pierrehumbert, Mark Branson, David Pollard, Daniel D. B. Koll

Robust elements of Snowball Earth atmospheric circulation and oases for life

Dorian S. Abbot,[1] Aiko Voigt,[2] Dawei Li,[1] Guillaume Le Hir,[3]
Raymond T. Pierrehumbert,[1] Mark Branson,[4] David Pollard,[5] and Daniel D. B. Koll[1]

Received 18 March 2013; revised 8 May 2013; accepted 31 May 2013; published 18 June 2013.

[1] Atmospheric circulation in a Snowball Earth is critical for determining cloud behavior, heat export from the tropics, regions of bare ice, and sea glacier flow. These processes strongly affect Snowball Earth deglaciation and the ability of oases to support photosynthetic marine life throughout a Snowball Earth. Here we establish robust aspects of the Snowball Earth atmospheric circulation by running six general circulation models with consistent Snowball Earth boundary conditions. The models produce qualitatively similar patterns of atmospheric circulation and precipitation minus evaporation. The strength of the Snowball Hadley circulation is roughly double modern at low CO_2 and greatly increases as CO_2 is increased. We force a 1-D axisymmetric sea glacier model with general circulation model (GCM) output and show that, neglecting zonal asymmetry, sea glaciers would limit ice thickness variations to $\mathcal{O}(10\%)$. Global mean ice thickness in the 1-D sea glacier model is well-approximated by a 0-D ice thickness model with global mean surface temperature as the upper boundary condition. We then show that a thin-ice Snowball solution is possible in the axysymmetric sea glacier model when forced by output from all the GCMs if we use ice optical properties that favor the thin-ice solution. Finally, we examine Snowball oases for life using analytical models forced by the GCM output and find that conditions become more favorable for oases as the Snowball warms, so that the most critical time for the survival of life would be near the beginning of a Snowball Earth episode.

Citation: Abbot, D. S., A. Voigt, D. Li, G. Le Hir, R. T. Pierrehumbert, M. Branson, D. Pollard, and D. D. B. Koll (2013), Robust elements of Snowball Earth atmospheric circulation and oases for life, *J. Geophys. Res. Atmos.*, *118*, 6017–6027, doi:10.1002/jgrd.50540.

1. Introduction

[2] At least three global-scale glaciations occurred during the Neoproterozoic at ≈715 Ma (Sturtian), ≈635 Ma (Marinoan), and ≈580 Ma (Edicaran) [*Hoffman and Li*, 2009]. Both the Sturtian and Marinoan glaciation show strong evidence for ice flowing from land into the ocean in tropical latitudes with carbonate sequences overlying glacial sequences. In addition, numerous banded iron formations, which represent possible evidence for global glaciation, are found in the Sturtian glaciation, but not generally in the others. U-Pb zircon radiometric dating suggests that the Sturtian glaciation may have lasted for as much as 70 Myr, the Marinoan for up to 20 Myr, and the Edicaran for a few million years [*Hoffman and Li*, 2009]. In addition, other global or nearly global glaciations, for which less data are available, occurred in the Paleoproterozoic (at ≈2.2 Ga [*Hoffman and Schrag*, 2002]).

[3] The Snowball Earth hypothesis attempts to explain these global-scale glaciations, or at least the more severe ones. According to the Snowball Earth hypothesis, the entire ocean was covered with ice and there was extensive low-latitude continental glaciation for a few million years, during which time CO_2 from volcanic outgassing built up to high enough values to melt tropical ice and reverse the global glaciation [*Kirschvink*, 1992; *Hoffman et al.*, 1998]. Alternative hypotheses have been suggested to explain Neoproterozoic glaciations, or at least the less severe ones, in which low-latitude continental glaciation occurred without the ocean completely freezing over [*Hyde et al.*, 2000; *Chandler and Sohl*, 2000; *Peltier et al.*, 2007; *Micheels and Montenari*, 2008; *Liu and Peltier*, 2010; *Abbot et al.*, 2011; *Yang et al.*, 2012a, 2012b], but we will consider the traditional (sometimes called "hard") Snowball Earth hypothesis here. The main outstanding theoretical questions for the Snowball Earth hypothesis are as follows: (1) What caused

[1]Department of the Geophysical Sciences, University of Chicago, Chicago, Illinois, USA.
[2]Max Planck Institute for Meteorology, Hamburg, Germany.
[3]Institut de Physique du Globe de Paris, Université Paris 7-Denis Diderot, Paris, France.
[4]Department of Atmospheric Science, Colorado State University, Fort Collins, Colorado, USA.
[5]Earth and Environmental Systems Institute, College of Earth and Mineral Sciences, Pennsylvania State University, University Park, Pennsylvania, USA.

Corresponding author: D. S. Abbot, Department of the Geophysical Sciences, University of Chicago, Chicago, IL 60637, USA. (abbot@uchicago.edu)

2169-897X/13/10.1002/jgrd.50540

Table 1. The Models Used in This Study, Their Version, Horizontal Resolution, Number of Vertical Levels Used, and Appropriate References[a]

Model	Version	Lon × Lat Res.	Vert. Levels	Reference(s)
FOAM	1.5	7.5° × 4.5°	18	*Jacob* [1997]
CAM	3.5	2.81° × 2.81°	30	*Collins et al.* [2004]
SP-CAM		2.81° × 2.81°	30	*Khairoutdinov and Randall* [2001] *Khairoutdinov et al.* [2008]
LMDz	4	5° × 3.83°	19	*Hourdin et al.* [2006]
ECHAM	6	1.88° × 1.88°	47	*Stevens et al.* [2013]
GENESIS	3	3.75° × 3.75°	18	*Thompson and Pollard* [1997] and *Alder et al.* [2011]

[a]The models are as follows: Community Atmosphere Model (CAM), Super Parameterized Community Atmosphere Model (SP-CAM), Laboratoire de Météorologie Dynamique-Zoom (LMDz), European Centre HAmburg Model (ECHAM), and Global ENvironmental and Ecological Simulation of Interactive Systems (GENESIS). Version 3 of GENESIS is similar to version 2, fully described by *Thompson and Pollard* [1997], but uses solar and thermal radiation codes from NCAR CCM3 and can optionally be coupled to the MOM2 ocean GCM [*Alder et al.*, 2011].

Snowball Earth events? (2) Can a Snowball Earth deglaciate at a reasonable CO_2 level? and (3) How did life survive Snowball Earth events? The first question is not considered here (see *Tziperman et al.* [2011], *Yang et al.* [2012a, 2012b, 2012c], *Voigt and Marotzke* [2010], *Voigt et al.* [2011], and *Voigt and Abbot* [2012] for recent work on this problem), as we assume Snowball Earth conditions in our calculations.

[4] The question of whether a Snowball Earth could deglaciate at a realistic CO_2 level was raised by early general circulation model (GCM) simulations [*Pierrehumbert*, 2004, 2005], which led to theories implicating albedo reduction through volcanic or aeolian dust [*Le Hir et al.*, 2010; *Abbot and Pierrehumbert*, 2010; *Abbot and Halevy*, 2010]. In a companion paper [*Abbot et al.*, 2012], we showed that clouds could warm a Snowball climate by ≈10 K, which would reduce the CO_2 needed for deglaciation by at least an order of magnitude. In the current paper, we focus on atmospheric circulation and the hydrological cycle in a Snowball. The mechanism for optically thick cloud formation in a Snowball identified by *Abbot et al.* [2012] was lifting of air by a vigorous Hadley circulation, which makes understanding the Snowball atmospheric circulation important. Moreover, atmospheric circulation in the Snowball determines heat export from the tropics to higher latitudes, which is crucial for the Snowball deglaciation threshold. Additionally, atmospheric circulation produces the precipitation minus evaporation pattern, which augments the flow of thick, floating "sea glaciers" on the Snowball ocean [*Goodman and Pierrehumbert*, 2003; *Pollard and Kasting*, 2005; *Goodman*, 2006; *Li and Pierrehumbert*, 2011; *Tziperman et al.*, 2012]. Sea glaciers flow strongly toward the equator because annual mean evaporation exceeds precipitation in the tropics in the Snowball as a result of annual mean descent in the tropics [*Pierrehumbert*, 2005; *Abbot and Pierrehumbert*, 2010]. Over hundreds of thousands of years, this would tend to concentrate surface dust in the tropics where it would be most important for deglaciation [*Abbot and Pierrehumbert*, 2010; *Li and Pierrehumbert*, 2011].

[5] Assuming global ice coverage, sea glaciers are expected to grow to a thickness of hundreds of meters, which would prevent photosynthetic activity in underlying oceans. Given this, two alternatives have been proposed to explain the survival of photosynthetic marine life through Snowball Earth events. The first proposal is that life survived in some small oases, possibly associated with volcanic activity [e.g., *Hoffman and Schrag*, 2000]. *Campbell et al.* [2011] considered whether oases could exist in narrow channels, into which sea glacier flow would be reduced by friction with the side walls. Similarly, *Tziperman et al.* [2012] considered the potential for oases in seaways constricted by a narrow entrance. These oases become more viable at lower ice temperature and higher evaporation minus precipitation. The second proposal for the survival of life is that the tropical net ablation zone, which is driven by atmospheric circulation, could lead to a Snowball solution with tropical ice thin enough that photosynthesis could occur beneath it [*McKay*, 2000; *Pollard and Kasting*, 2005]. We will consider both types of oases here. This paper therefore addresses how the atmospheric circulation affects both the CO_2 threshold for Snowball deglaciation and the survival of life through Snowball Earth episodes.

[6] GCMs are the main tools we have to make detailed predictions about atmospheric temperature, circulation, precipitation, and evaporation in a Snowball Earth, and they have been applied to the problem of global glaciation at least since *Wetherald and Manabe* [1975]. Because GCMs have not always yielded consistent results in Snowball conditions, detailed comparisons between GCMs are required to determine robust predictions. Initial efforts to compare GCMs run in Snowball situations have been performed by *Le Hir et al.* [2007, 2010], *Abbot and Pierrehumbert* [2010], *Hu et al.* [2011], *Pierrehumbert et al.* [2011], and *Abbot et al.* [2011]. Preliminary results suggest that models simulate atmospheric circulation of consistent pattern, but widely varying strength, under Snowball conditions [*Abbot and Pierrehumbert*, 2010; *Hu et al.*, 2011]. In this paper and its companion [*Abbot et al.*, 2012], we perform a rigorous comparison of GCMs (Table 1) run in a consistent Snowball Earth configuration. In the Snowball Earth hypothesis CO_2 accumulates throughout the event, so we run the models at $CO_2 = 10^{-4}$ (10^2 ppm), as a proxy for early Snowball conditions, and at $CO_2 = 0.1$ (10^5 ppm), as a proxy for a nearly deglaciating Snowball.

[7] This paper is organized as follows. In section 2 we describe the models and simulations. We highlight the important results from these simulations in section 3. In particular, we find that the pattern of atmospheric circulation and precipitation minus evaporation are consistent across the models, although the magnitude of the stream function maximum differs by up to 100% among models. This confirms that the shape of the hydrological forcing of sea glacier flow is a robust feature of Snowball Earth simulation. We also find

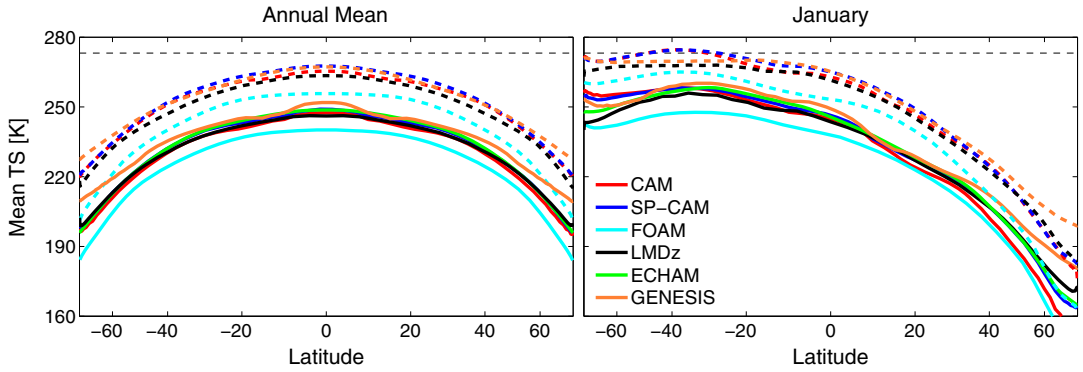

Figure 1. (left) Annual and (right) January zonal mean surface temperature for the GCMs run with $CO_2 = 10^{-4}$ (thick solid lines) and $CO_2 = 0.1$ (thick dashed lines). The thin dashed black line denotes the melting temperature of pure ice. The surface albedo is set to 0.6 in these simulations, so we neglect the effect of snow and dust on the surface albedo.

that differences in model cloud simulation are much more important than differences in heat export from the tropics for determining the Snowball deglaciation threshold. We consider sea glacier flow and oasis solutions in section 4. We find that sea glacier flow is efficient enough when forced by output from all GCMs to make sea glacier thickness fairly uniform and that oases become increasingly favorable as the Snowball ages and warms, mostly due to the reduction in sea glacier thickness outside of the oasis region. We summarize our conclusions in section 5.

2. Brief Description of Models and Simulation Specifications

[8] We provide a brief description of the simulations here. Readers interested in more detail should consult the supplementary material of *Abbot et al.* [2012]. We run General Circulation Models (GCMs) FOAM, CAM, LMDz, ECHAM, and GENESIS (Table 1) for 10 years and average results over the final 5 years. SP-CAM contains a numerically expensive embedded cloud resolving scheme, so we initialize SP-CAM simulations from converged CAM simulations, run them for 2 years, and average variables over the final year. We run each model with $CO_2 = 10^{-4}$ and $CO_2 = 0.1$ (10^5 ppm), and we have validated the radiation schemes to within 2 W m^{-2} at $CO_2 = 0.1$ [*Abbot et al.*, 2012]. ECHAM only contributes to the $CO_2 = 10^{-4}$ simulation because it becomes unstable when CO_2 is increased to 0.1.

[9] To avoid ice vertical resolution issues [*Abbot et al.*, 2010], we set the land surface to "glacial ice," like Greenland and Antarctica in modern simulations, everywhere. This is roughly equivalent to assuming that all continents are covered with low-elevation land ice. We initialize snow cover at zero everywhere. We set the surface albedo to 0.6 everywhere, for both snow and glacial ice, regardless of temperature and age. This allows comparison of atmospheric behavior among models without introducing surface albedo differences due to different simulation of snow cover. We set the solar constant to 1285 W m^{-2} (94% of its present value) and set the radiative effect of all aerosols to zero, thereby neglecting potential dust aerosol radiative forcing [*Abbot and Halevy*, 2010]. To minimize simulation differences among models, we set ozone and all greenhouse gases other than CO_2 and H_2O to zero. For the warmer simulations with tropopause heights of ≈15 km, setting ozone to zero could increase the tropopause height by a few kilometers [*Thuburn and Craig*, 1997]. We set the obliquity to 23.5° and the eccentricity to 0.

3. Simulation Results

3.1. Review of Temperature

[10] The models show a similar meridional surface temperature distribution (Figure 1). The surface temperatures of all models except FOAM cluster within about 5 K, and FOAM is about 10 K colder than the other models. This is due to extremely low cloud condensate simulation in FOAM, such that clouds have very little radiative effect [*Abbot et al.*, 2012]. Since snow has a higher albedo than 0.6, the temperature of a Snowball Earth would likely be lower than that depicted in Figure 1 in snow-covered regions. Similarly, the temperature would be lower in regions made darker by the mixture of dust with snow and ice [*Le Hir et al.*, 2010; *Abbot and Pierrehumbert*, 2010]. At both $CO_2 = 10^{-4}$ and 0.1, all models produce strong inversions in the winter hemispheres (Figure 2), and in the annual mean, the atmosphere in all models is highly stable poleward of about 30° (not shown). This results from an annual cycle in which a region of convection tracks the insolation maximum and the atmosphere is stable elsewhere. The temperature inversion in the winter extratropical profile is a basic feature of the Snowball climate that was identified in FOAM [*Pierrehumbert*, 2004, 2005] and is now seen to be robust across other models. This inversion is important because the greenhouse effect is greatly reduced if the atmospheric emission temperature approaches the surface temperature.

3.2. Hadley Cell Strength and Heat Export From Tropics

[11] In this paper we are primarily interested in tropical cloud formation, heat export out of the tropics, and the tropical net ablation zone, because of their effects on deglaciation and sea glacier flow. Because all of these factors are to a large extent governed by the tropical mean meridional circulation, we will focus on the Hadley cell here.

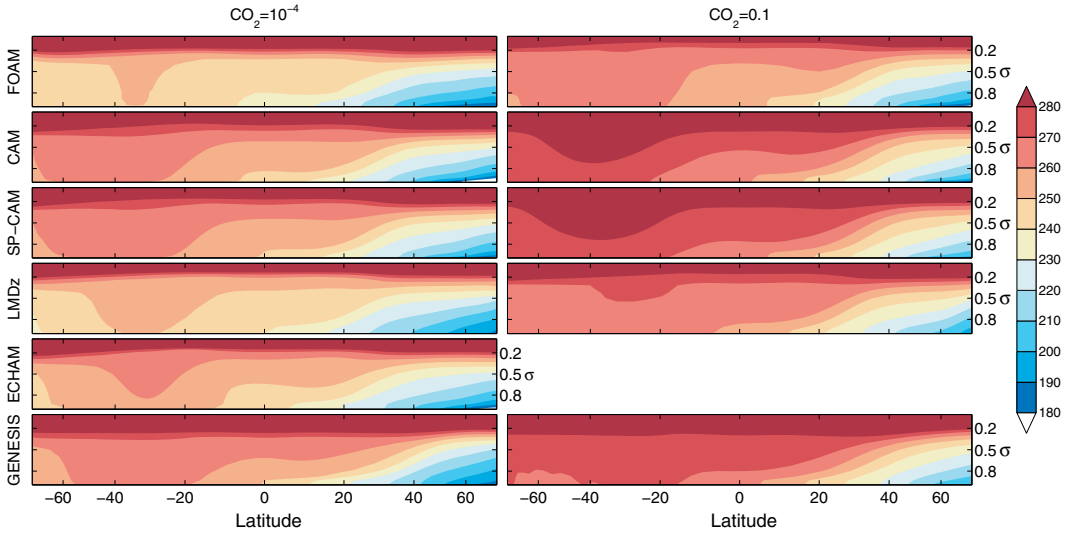

Figure 2. Zonal mean January potential temperature for the models. $\sigma = \frac{P}{P_s}$ is the pressure normalized by the surface pressure.

The primary purpose of this section is to compare circulation results from the GCMs we have run and to outline potential explanations. Further research with a hierarchy of models would be required to fully resolve the relative contribution of the effects we discuss here.

[12] The pattern of zonal-mean Snowball atmospheric general circulation (Figures 3 and 4) is similar among the models. In the annual mean, the tropical circulation is thermally indirect (Figure 3), with descent where heating is highest. As described by *Abbot and Pierrehumbert* [2010], the cause of this thermally indirect net circulation is the low surface heat capacity of ice, which allows the region of maximum upwelling to deviate far from the equator (Figure 4) so that the two solstitial circulation patterns dominate the annual mean. We will therefore focus on understanding the solstitial circulation in what follows. Increasing CO_2 from 10^{-4} to 0.1 does not substantially change the width of the circulation, but does increase the circulation depth.

[13] The models produce much stronger circulation with Snowball boundary conditions than in the modern climate. For example, the maximum January stream function is 2–4 times the modern value of $\approx 160 \times 10^9$ kg s^{-1} [*Dima and Wallace*, 2003] at $CO_2 = 10^{-4}$ and 4–6 times stronger at $CO_2 = 0.1$ (Table 2). The main reason for this is the monsoon-like behavior of the Snowball Hadley circulation. Because of the low heat capacity, the maximum surface temperature in January is at ≈30–35°S (Figure 1). This means that the effective heating of the atmosphere is delivered far off the equator, which significantly enhances the strength of the Hadley circulation [*Lindzen and Hou*, 1988;

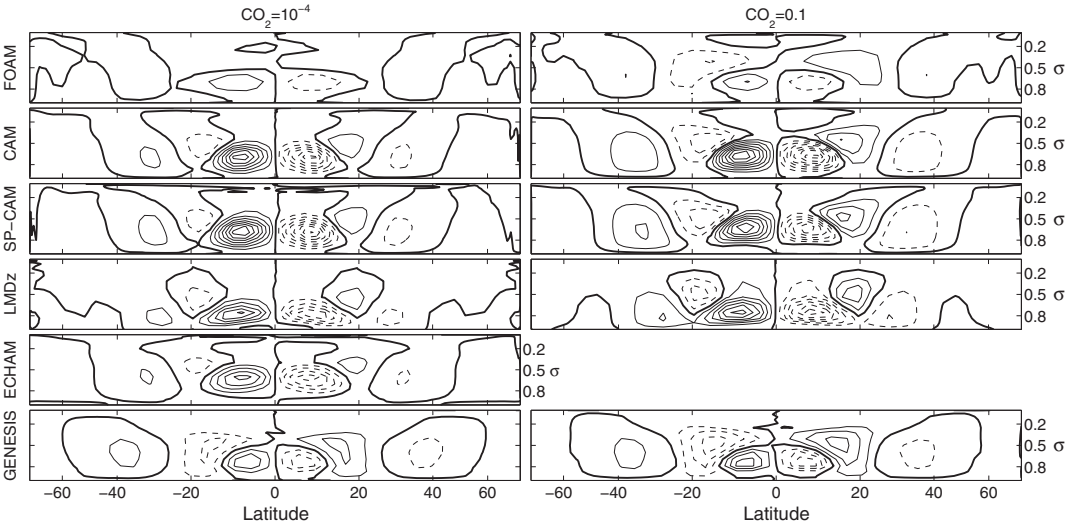

Figure 3. Annual mean mass Eulerian stream function for the models. Clockwise circulation is depicted by thin solid lines, counterclockwise circulation is depicted by thin dashed lines, and the zero stream function contour is thick and solid. Contour spacing is 20×10^9 kg s^{-1}. All models show annual mean descent in the deep tropics. Maximum stream function values for each model are given in Table 2.

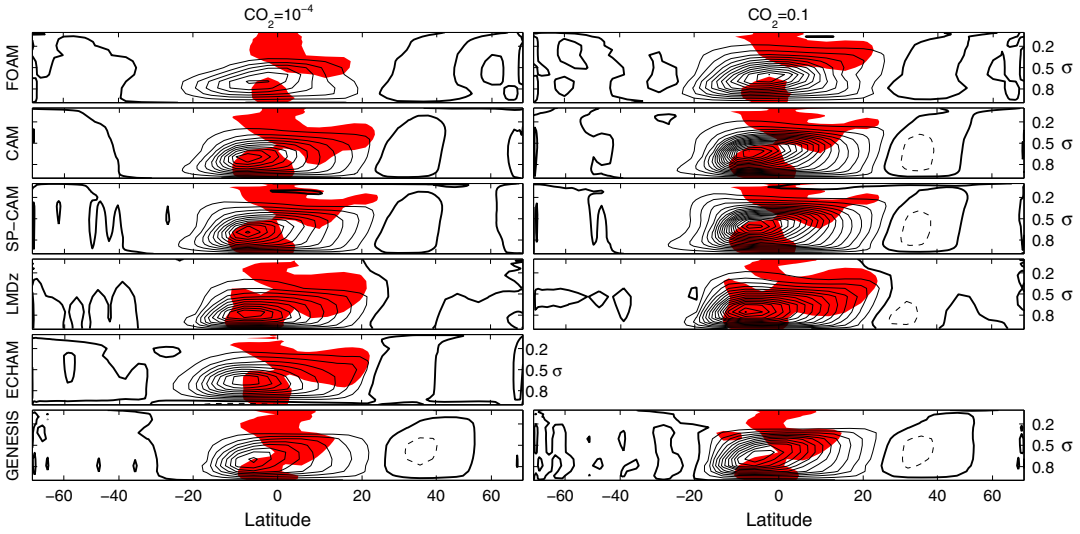

Figure 4. January mean mass Eulerian stream function for the models. Clockwise circulation is depicted by thin solid lines, counterclockwise circulation is depicted by thin dashed lines, and the zero stream function contour is thick and solid. Contour spacing is 50×10^9 kg s^{-1}. Maximum stream function values for each model are given in Table 2. The region where the local Rossby number is greater than 0.5 is shaded red. The local Rossby number is defined as $Ro \equiv \frac{\frac{\partial}{\partial\theta}(\bar{u}\cos\theta)}{2\Omega a \sin\theta\cos\theta}$, where a is the Earth's radius, Ω is the Earth's rotation rate, θ is the latitude, and $\bar{u}$ is the zonal mean zonal velocity.

Fang and Tung, 1996; *Walker and Schneider*, 2005; *Schneider and Bordoni*, 2008]. Another major contributor to the strong Snowball Hadley circulation is the lack of ocean heat transport in a Snowball climate. In the modern climate, both the atmosphere and ocean can transport heat from the summer to winter hemisphere in solstitial conditions. In the Snowball, there is no ocean to transport heat, and the atmosphere responds by increasing the heat it transports through increasing the Hadley cell strength. In a variety of models run in modern conditions, decreasing the ocean heat transport from its present value to zero roughly doubles the strength of the annual mean Hadley circulation [*Herweijer et al.*, 2005; *Winton*, 2003; *Barreiro et al.*, 2011; *Rose and Ferreira*, 2013], which demonstrates how much removing ocean heat transport can increase atmospheric circulation. Finally, we note that there are other factors that likely work against the increase in Hadley cell strength in a Snowball relative to modern, such as the increased global mean albedo, which would tend to decrease planetary heat transport [*Stone*, 1978].

[14] A robust feature of all the GCMs in this study is an increase in circulation strength with increasing CO_2 (Table 2), which is consistent with previous work [*Pierrehumbert*, 2005; *Hu et al.*, 2011]. As a first step to qualitatively understand this, we apply the axisymmetric angular-momentum-conserving model of *Held and Hou* [1980], which yields qualitatively similar parameter scalings as eddy-dominated theories [*Walker and Schneider*, 2006; *Schneider*, 2006], although with different power laws. Consideration of the local Rossby number (the local ratio of relative to planetary vorticity) suggests that the angular-momentum-conserving limit is a reasonable starting point when considering the Snowball circulation. The angular-momentum-conserving limit corresponds to a local Rossby number in the upper branch of the Hadley cell near one [*Walker and Schneider*, 2006], and it is greater than 0.5 in our simulations (Figure 4) and does not change much as CO_2 is increased.

[15] Following *Schneider* [2006] and *Held and Hou* [1980] theory yields a stream function maximum (Ψ_{max}) that scales as

$$\Psi_{max} \sim \rho_0 \frac{a^2 H}{\tau}\left(\frac{gH}{\Omega^2 a^2}\frac{\Delta_h}{T_0}\right)^{\frac{3}{2}}\frac{\Delta_h}{\Delta_v}, \quad (1)$$

where ρ_0 is the reference density, g is the gravitational acceleration, Ω is the planetary rotation rate, H is the height of the tropopause, τ is the radiative timescale (relaxation time to radiative-convective equilibrium), T_0 is the reference surface temperature, Δ_h is the difference between the surface

Table 2. Annual and January Maximum Mass Stream Functions Measured in 10^9 kg s^{-1} at Both $CO_2 = 10^{-4}$ and $CO_2 = 0.1$[a]

Model	Annual, $CO_2 = 10^{-4}$	Annual, $CO_2 = 0.1$	January, $CO_2 = 10^{-4}$	January, $CO_2 = 0.1$
FOAM	39.3	41.8	307.8	651.7
CAM	132.1	153.4	548.1	900.2
SP-CAM	158.2	139.0	611.4	928.7
LMDz	105.1	129.5	547.0	803.6
ECHAM	86.6	—	475.5	—
GENESIS	59.1	65.0	413.0	640.4

[a]Note that the tropical circulation is thermally indirect in the annual mean (Figure 3).

Table 3. Held and Hou Model Parameters[a]

Model	H_0 [km]	δH [km]	Δ_{v0} [K]	$\delta\Delta_v$ [K]	Δ_{h0} [K]	$\delta\Delta_h$ [K]
FOAM	8	+6.3	19	+24.0	62	+1.5
CAM	11	+4.7	42	+18.6	66	-8.3
SP-CAM	12	+3.9	45	+6.6	61	-0.9
ECHAM	12	—	48	—	62	—
LMDz	10	+2.1	30	+1.6	57	-2.0
GENESIS	10	+8.1	38	+53.6	58	-3.7

[a]The tropopause height at the equator in January defined using a 4 K km^{-1} lapse rate criterion [*Voigt et al.*, 2012] at $CO_2 = 10^{-4}$ (H_0), the change in tropopause height when CO_2 is increased from 10^{-4} to 0.1 (δH), the difference between the potential temperature at the tropopause and the surface (stability) in January at the equator at $CO_2 = 10^{-4}$ (Δ_{v0}), the change in stability when CO_2 is increased from 10^{-4} to 0.1 ($\delta\Delta_v$), the difference in surface temperature between a latitude of 20°S and 50°N in January at $CO_2 = 10^{-4}$ (Δ_{h0}), and the change in Δ_{h0} when CO_2 is increased from 10^{-4} to 0.1 ($\delta\Delta_h$). We choose the latitude range for Δ_{h0} to extend roughly from the January surface temperature maximum to where differences in simulation of the winter temperature inversion cause large divergences in surface temperature simulation among the models. Note that we calculate the values of Δ_v and Δ_h after equilibration with atmospheric dynamics, because this is what we have, rather than the values of an imagined forcing temperature field, which is what would be required for strict consistency with *Held and Hou* [1980]. The tropopause height calculated here corresponds roughly to where the mass stream function approaches zero. The calculated tropopause height is quantitatively similar if a lapse rate criterion between 3–5 K km^{-1} is used and qualitatively similar if a lapse rate criterion between 2–6 K km^{-1} is used.

temperature at the equator and the pole of a forcing temperature field, and Δ_v is the difference between the potential temperature at the surface and the upper branch of the Hadley cell (gross stability). *Fang and Tung* [1996] find a similar scaling as *Held and Hou* [1980] with maximum heating off the equator rather than symmetric forcing. As CO_2 is increased, tropopause height, which increases by 20–100%, is the only variable in equation (1) that changes in the right direction to increase circulation when CO_2 is increased from 10^{-4} to 0.1 (Table 3). Based on equation (1), this increase in tropopause height is enough to explain the increase in circulation strength with CO_2. Large increases in tropopause height are reasonable given the increase in surface temperature and emission height that the models experience when CO_2 is increased [*Schneider et al.*, 2010], even if water vapor changes are minimal [*Thuburn and Craig*, 1997].

[16] Although *Held and Hou* [1980] theory provides a reasonable explanation for the increase in circulation strength with CO_2 (via tropopause height), it would also predict an increase in circulation extent, which we do not observe (Figure 4). This suggests that other effects may also be important. For example, idealized GCM simulations suggest that for global mean temperatures below freezing, moist dynamical effects lead to strong increases in Hadley cell strength with temperature [*O'Gorman and Schneider*, 2008].

[17] The GCMs show roughly 100% variation in circulation strength at $CO_2 = 10^{-4}$ and 50% variation at $CO_2 = 0.1$ (Table 2). *Held and Hou* [1980] theory (equation (1)) cannot simply explain this based on variation in relevant parameters among models (Table 3). A more likely explanation lies in differences in model simulation of vertical momentum transport by dry turbulence, which *Voigt et al.* [2012] showed can cause $\mathcal{O}(1)$ variations in Snowball Hadley cell strength. Confirming this would require repeating the analysis of *Voigt et al.* [2012] for solstitial rather than equinoctial conditions and making a detailed study of the parameterization of vertical momentum transport in the GCMs.

[18] An important impact of the atmospheric circulation is heat export from the tropics, which affects tropical surface temperatures and the CO_2 threshold for deglaciation. As shown in *Abbot et al.* [2012], differences in cloud simulation are the main cause of tropical surface temperature differences among models. Models with higher tropical cloud radiative forcing (CRF) are warmer and show a somewhat higher heat export to higher latitudes (Table 4). For most models, differences in heat export are much smaller than differences in CRF, but higher heat export for warmer models does decrease somewhat temperature differences caused by differences in CRF. Heat export from the tropics is exceptionally large in GENESIS, and this appears to be the main factor keeping the tropical surface temperature only a few degrees warmer than the other models despite a much higher CRF. All models show a small increase in heat export as the CO_2 is increased from 10^{-4} to 0.1. Heat export therefore forms a robust but small negative feedback that works against deglaciation. In contrast, CRF changes with CO_2 are also small, but their sign is not consistent across models.

3.3. Similarity of Hydrological Cycle Pattern Among Models

[19] Precipitation minus evaporation (or sublimation) is driven by atmospheric circulation. Mean descent tends to lead to evaporation exceeding precipitation and mean ascent leads to the opposite. The pattern of precipitation minus evaporation is robust across models, with a broad region of net ablation in the tropics (Figure 5). The amount by which evaporation exceeds precipitation in the tropics increases with CO_2, due to increased circulation strength (see below) and warmer air, which can hold more moisture. Differences in the magnitude of the precipitation minus evaporation

Table 4. Tropical (20°S to 20°N) Surface Temperature (TS), Top-of-Atmosphere Cloud Radiative Forcing (CRF), and Heat Export to Higher Latitudes (Absorbed Shortwave Radiation Minus Outgoing Longwave Radiation in the Tropics) for Each Model

Model	CO_2	TS [K]	CRF [W m^{-2}]	Heat Export [W m^{-2}]
FOAM	10^{-4}	238.9	1.2	6.7
CAM	10^{-4}	244.9	14.5	10.8
SP-CAM	10^{-4}	246.5	18.8	11.3
LMDz	10^{-4}	244.6	11.3	10.3
ECHAM	10^{-4}	247.1	20.5	12.1
GENESIS	10^{-4}	248.1	35.1	23.4
FOAM	0.1	254.8	1.9	11.9
CAM	0.1	263.5	11.4	18.0
SP-CAM	0.1	266.0	17.1	18.4
LMDz	0.1	261.7	14.6	16.7
GENESIS	0.1	265.3	39.7	29.4

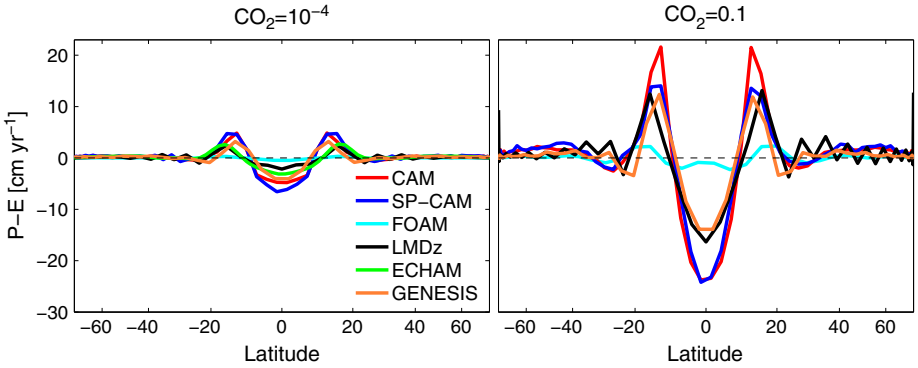

Figure 5. Annual and zonal mean precipitation minus sublimation or evaporation with (left) $CO_2 = 10^{-4}$ ppm and (right) $CO_2 = 0.1$. All models show evaporation exceeding precipitation in the deep tropics. The hydrological cycle in FOAM is muted due to cold surface temperatures. LMDz exhibits grid scale noise in precipitation minus evaporation at CO_2=0.1.

pattern are largely driven by differences in model temperature. Additionally, all of the models show a small region in the subtropics where evaporation exceeds precipitation, which we will return to when discussing the thin-ice Snowball model (section 4.3). The subtropical net ablation zone is due to moisture flux out of the subtropics by midlatitude eddies and is stronger and larger in GCMs that produce warmer and moister conditions.

[20] Based on simulations using an ice sheet model driven by output from the LMDz GCM, *Donnadieu et al.* [2003] argued that the hydrological cycle during a global glaciation would be sufficiently strong to produce the observed evidence of flowing continental glaciers. Measured by precipitation minus evaporation extrema, all models except FOAM simulate a hydrological cycle at least as strong as LMDz (Figure 5). Measured by total global evaporation (latent heat), all models simulate a hydrological cycle stronger than LMDz (not shown). This suggests that the conclusions of *Donnadieu et al.* [2003] should be robust to changing the GCM driving the glacial model.

4. Sea Glacier Flow

4.1. Axisymmetric Flow Makes Sea Glacier Thickness Uniform

[21] In a Snowball Earth, thick "sea glaciers" that could flow viscously would be expected to form on the surface of the ocean, rather than the thin sea ice that forms in polar regions of the modern climate [*Goodman and Pierrehumbert*, 2003]. The flow of these glaciers would be driven by surface temperature, precipitation, and evaporation patterns. As a preliminary means of investigating the effect of the climate simulated by the different GCMs on sea glacier flow, we run the one-dimensional (latitude) axisymmetric model of *Goodman and Pierrehumbert* [2003] with a uniform geothermal heat flux of 0.08 W m^{-2}. We use the code of *Li and Pierrehumbert* [2011], which fixes a programming error contained in *Goodman and Pierrehumbert* [2003]. A zonally symmetric model is appropriate for the zonally symmetric boundary conditions we apply to the GCMs, but will not capture ice thickness variations due to heterogeneity introduced by continents [*Campbell et al.*, 2011; *Tziperman et al.*, 2012]. Additionally, in this section, we neglect solar radiation absorption by transmission through the ice and, therefore, do not consider the tropical thin ice Snowball solutions proposed by *McKay* [2000] and *Pollard and Kasting* [2005].

[22] Consistent with the results of *Li and Pierrehumbert* [2011] and *Tziperman et al.* [2012], zonally symmetric sea glacier flow is efficient and leads to variation in ice thickness of only $\mathcal{O}(10\%)$ or less when forced by output from all of the GCMs (Figure 6). In steady state, the global mean of the equation for mass conservation of ice [*Li and Pierrehumbert*, 2011; *Tziperman et al.*, 2012] simplifies to

$$F_g = \left\langle \frac{k(T_f - T_s(\theta))}{h(\theta)} \right\rangle,$$

where θ is the latitude, $h(\theta)$ is the ice thickness, k is the thermal conductivity of ice, T_f is the freezing point of water, $T_s(\theta)$ is the surface temperature at the top of the ice, and $\langle x \rangle$

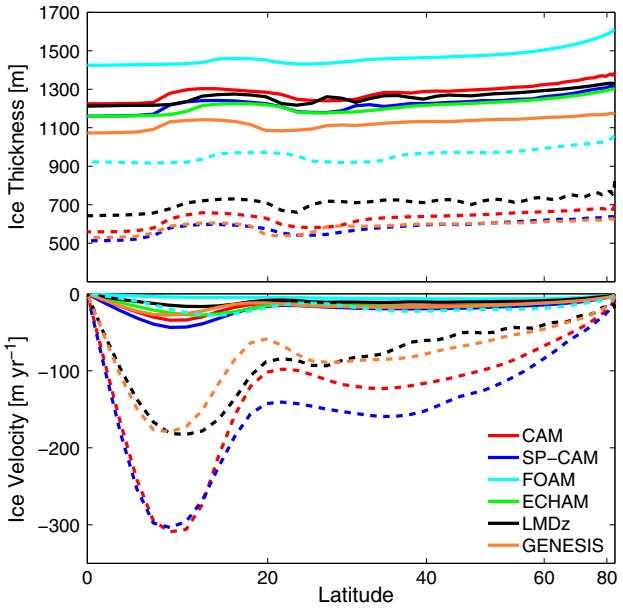

Figure 6. (top) Ice thickness and (bottom) ice meridional velocity calculated using the one-dimensional (latitude) sea glacier model of *Li and Pierrehumbert* [2011] for the GCMs.

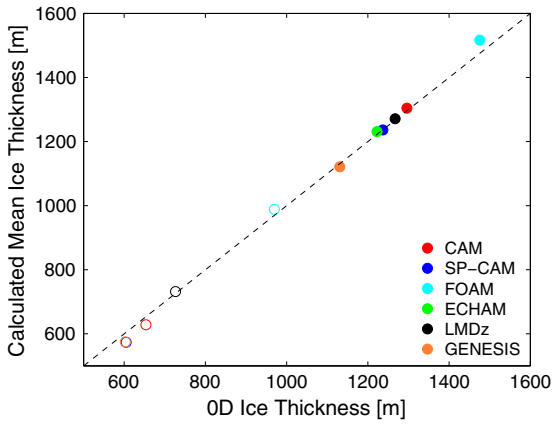

Figure 7. Comparison of the approximate mean ice thickness calculated using the mean surface temperature (equation (2)) with the mean ice thickness calculated using the 1-D ice flow model.

is the global mean of a variable x. If variations in $h(\theta)$ are small, then

$$\left\langle \frac{k(T_f - T_s(\theta))}{h(\theta)} \right\rangle \approx \frac{k(T_f - \langle T_s(\theta) \rangle)}{\langle h(\theta) \rangle},$$

which yields

$$\langle h(\theta) \rangle \approx \frac{k(T_f - \langle T_s(\theta) \rangle)}{F_g}, \tag{2}$$

i.e., the average ice thickness can be estimated by the thickness that would result from a 0-D ice thickness model with the surface temperature set to the hemispheric mean surface temperature. We find that this is a very good approximation for the mean ice thickness in the simulations (Figure 7).

[23] The picture that emerges from these 1-D sea glacier flow simulations, therefore, is that, for all GCMs and at both CO_2 values, ice flow is efficient enough that sea glacier thickness is effectively uniform. This thickness is then simply determined by the global mean surface temperature. Even in the warmest models at $CO_2 = 0.1$, the ice thickness is still 2 orders of magnitude larger than 5–10 m (Figure 7), which is what would be required for photosynthesis underneath ice [*McKay*, 2000; *Pollard and Kasting*, 2005].

4.2. "Thin Ice" Solution Possible for Certain Optical Properties

[24] A potential explanation for the apparent survival of photosynthetic life through Snowball Earth episodes is regions of ice thin enough to allow sunlight to pass through it [*McKay*, 2000; *Pollard and Kasting*, 2005]. This might be possible in snow-free regions (e.g., the tropics) if the ice can transmit and absorb enough energy to warm and thin it sufficiently. There is, however, significant debate about whether ice with properties that would allow it to be sufficiently thin is possible [*Warren et al.*, 2002; *Warren and Brandt*, 2006; *Pollard and Kasting*, 2006]. Moreover, meteoric ice formed by compaction of snow at higher latitudes, which is much more reflective and less transmissive of sunlight than marine ice formed by freezing seawater, could be advected by sea glacier flow into net ablation zones [*Goodman*, 2006], preventing the formation of thin ice there. In this section, we will assume ice properties that favor the thin-ice Snowball and neglect differences between meteoric and marine ice, and repeat the axisymmetric sea glacier calculations of section 4.1. This will allow us to determine whether a thin-ice solution is possible for all the GCMs and at both low and high CO_2 using these optimistic assumptions.

[25] To calculate solar absorption in the ice, we assume exponential decay of solar flux with a penetration depth scale, h, in all ice that is not covered with snow [*McKay*, 2000]. *McKay* [2000] used $h = 0.8$ m, but *Warren et al.* [2002] argued that doing a proper spectral integral leads to a mean value closer to $h = 0.05$ m, which is the value *Goodman and Pierrehumbert* [2003] used. *Pollard and Kasting* [2005] used a two-stream model of solar penetration, but based on their Figure A2, the effective penetration depth is $h \approx 1.5$ m. We will use $h = 1$ m here, but still specify a surface albedo of 0.6 even for this highly transparent ice.

[26] Using these assumptions, we find that all GCMs produce ice thinner than 1 m in the tropics at both $CO_2 = 10^{-4}$ and 0.1 (Figure 8). The ice is thicker in colder GCMs and at lower CO_2 for a given GCM, but in all cases, it would be thin enough for photosynthesis to occur beneath the ice [*McKay*,

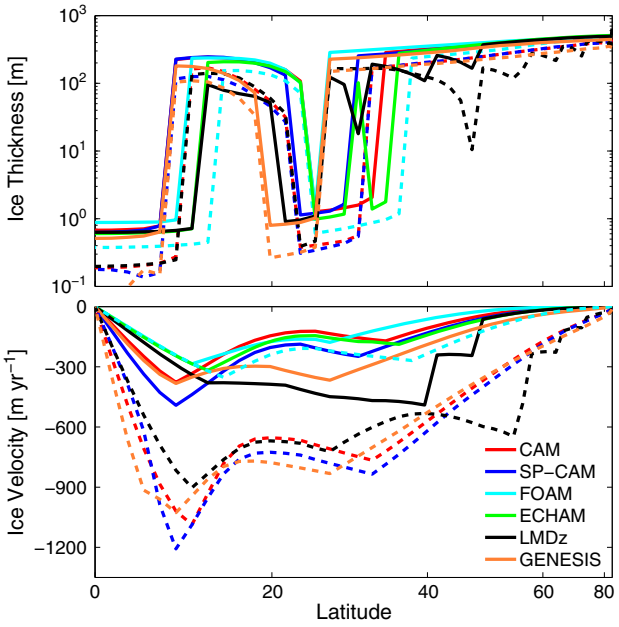

Figure 8. (top) Ice thickness and (bottom) ice meridional velocity calculated using the one-dimensional (latitude) sea glacier model of *Li and Pierrehumbert* [2011] for the GCMs including solar absorption in snow-free regions, assuming an exponential decay of solar flux with a penetration depth of 1 m. All models can produce a thin ice region using these solar absorption assumptions.

2000]. This demonstrates that the thin-ice Snowball solution including sea glacier flow [*Pollard and Kasting*, 2005] is robust to different GCM forcings, as long as favorable ice optical properties are used.

[27] In addition to the thin ice region in the tropics, all GCMs also produce a thin ice region in the subtropics (Figure 8), corresponding to the net ablation region caused by eddy moisture export to higher latitudes (Figure 5). The magnitude of evaporation minus precipitation is much smaller in this region than in the deep tropics, which would make this region of thin ice particularly susceptible to destruction by advection of meteoric ice. For example, if we assume a subtropical ice velocity scale of 100 m yr^{-1}, an evaporation minus precipitation of 0.01 m yr^{-1}, and a meteoric ice thickness of 100 m, then the meteoric ice can penetrate into the subtropical ablation zone on the order of 1000 km. Since this is on the order of the size of the subtropical net ablation zone, it might not be stable in a model including advection of meteoric ice. A full investigation of this effect would require a model that separates meteoric from marine ice, such as that used by *Goodman* [2006].

4.3. Oases Expand in a Warming Snowball

[28] The flow of sea glaciers into restricted spaces would be reduced, allowing the possibility of oases (ice thin enough for photosynthesis underneath) in net ablation zones. *Campbell et al.* [2011] developed an analytical solution for the penetration length of a sea glacier into a rectangular channel (like the Red Sea, but without Bab-el-Mandeb, the constriction at its entrance), and *Tziperman et al.* [2012] developed a scaling relation for the sea glacier height difference between the outside and inside of a constricted seaway (like the Mediterranean). At higher temperatures, ice is softer and flows more easily, which would tend to close off oases. Higher temperatures should also lead to larger evaporation minus precipitation in net ablation zones, which would tend to expand oases. Here we use the GCM results to consider the question of whether oases should tend to expand, remain stable, or close up as a Snowball warms over the course of its life cycle. This is a critical question, since an oasis would have to remain open through an entire Snowball to be a viable solution to the problem of the survival of marine photosynthetic and possibly animal life through Snowball Earth events.

[29] First, we consider the channel oasis of *Campbell et al.* [2011]. The ratio of the penetration length (L) to the channel width (W) is given by

$$\frac{L}{W} = \frac{H_0}{D}, \tag{3}$$

where H_0 is the sea glacier thickness at the entrance of the channel, and

$$D = \left(\frac{2^n (E-P)(n+2)}{\langle A(T) \rangle \Gamma^n} \right)^{\frac{1}{n+1}}, \tag{4}$$

where $\langle A(T) \rangle$ is the vertical average of the ice softness parameter, which describes the decrease in ice viscosity with increasing temperature and which we calculate as in *Campbell et al.* [2011]. n is the exponent in Glen's flow law, $\Sigma \propto \tau^n$, where Σ is the strain and τ is the stress. For a Newtonian fluid, $n = 1$. Ice is shear thinning, with $n \approx 3$, which is the value we will adopt. Γ is defined by

$$\Gamma = \rho_i g \left(1 - \frac{\rho_i}{\rho_w}, \right)$$

where ρ_i is the density of ice, ρ_w is the density of water, and g is gravitational acceleration. The slight difference between equations (4) and (14) in *Campbell et al.* [2011] is due to an error in that manuscript (A.J. Campbell, personal communication, 2012).

[30] We calculate $\frac{L}{W}$ using evaporation minus precipitation and surface temperature for all models at both CO_2 values. We find that conditions for oases are most favorable at the equator, which is a nontrivial result since E-P and surface temperature are in competition, and therefore only display $\frac{L}{W}$ values calculated there. For easier comparison among models, we set $H_0 = 1200$ m at $CO_2 = 10^{-4}$ and $H_0 = 600$ m at $CO_2 = 0.1$, which is roughly consistent with the equatorial sea glacier thicknesses in most models (Figure 6). *Campbell et al.* [2011] use the Red Sea, for which $\frac{L}{W} \approx 6.5$, as a reference for a potential oasis. They argue that if the penetration depth is less than about 6–7 times the channel width, there is a reasonable chance that such an oasis might have existed during a Snowball because we have a large example of such a channel on modern Earth. We find that for most of the models $\frac{L}{W} = 10 - 12$ at CO_2=10^{-4} (Table 5), so that a channel much more elongated than the Red Sea would be required for this type of oasis. The situation is significantly worse for a channel oasis when forced with FOAM output, as a result of a much lower evaporation minus precipitation at the equator (Figure 5), which overwhelms the ice stiffening due to colder temperatures. When CO_2 is increased to 0.1, we find that conditions become much more favorable for a channel oasis ($\frac{L}{W}$ is reduced, Table 5). This is mostly due to the reduction in H_0 for warmer temperatures and means that the most dangerous time for a channel oasis is early

Table 5. Calculations Relevant for Potential Oases for Life During a Snowball Based on Evaporation Minus Precipitation and Surface Temperature in the GCMs[a]

Model	$CO_2 = 10^{-4}$, $\frac{L}{W}$	$H_0 = 1200$ m ΔH	$CO_2 = 0.1$, $\frac{L}{W}$	$H_0 = 600$ m ΔH
FOAM	16.5	700	9.8	500
CAM	10.6	1200	4.6	1200
SPCAM	10.1	1300	4.7	1100
ECHAM	12.0	1000	—	—
LMDz	12.7	900	4.9	1100
GENESIS	11.8	1000	5.3	900

[a]GCM output at the equator is used for the calculations shown here, as this is the most favorable location for oases. H_0 is the sea glacier thickness outside of the oasis, and is set to a constant, which depends on CO_2 for all models. $\frac{L}{W}$ is the ratio of the penetration length to the channel width for the channel oasis described by *Campbell et al.* [2011], and is rounded to the nearest tenth. For reference, $\frac{L}{W} \approx 6.5$ for the Red Sea. ΔH is the difference between the sea glacier thickness outside and inside the constricted seaway oasis described by *Tziperman et al.* [2012], and is rounded to the nearest hundred. The scaling constant for the calculation of ΔH is chosen so that the sea glacier thickness is near zero at $CO_2 = 10^{-4}$. Both types of oases become more favorable at high CO_2, mostly because the ice thickness outside the oasis is reduced.

in the Snowball life cycle. The length scale D (equation 4) stays roughly constant as the climate warms, which can be explained by the similar value of the Clausius-Clapeyron exponent and the activation energy for ice creep [*Campbell et al.*, 2011].

[31] *Tziperman et al.* [2012] find that the thickness difference between the inside and outside of a constricted seaway (ΔH) should scale like

$$\Delta H \sim (E-P)^{\frac{1}{n}} \langle A(T)^{-\frac{1}{n}} \rangle. \quad (5)$$

Following *Tziperman et al.* [2012], we use $A(T)$ as given in *Goodman and Pierrehumbert* [2003], but find similar results when we use the formulae in *Campbell et al.* [2011], *Pollard and Kasting* [2005], and *Barnes et al.* [1971]. The proportionality constant inequation (5) is affected by factors such as the geometry of the seaway. We choose this constant so that $\Delta H \approx H_0$ at $CO_2 = 10^{-4}$ for most models, which is equivalent to assuming that a constricted seaway oasis is possible. We then find that ΔH stays roughly constant when we repeat the calculation using GCM output at $CO_2 = 0.1$, which is similar to the behavior of D in the channel oasis case. Since H_0 is significantly reduced as CO_2 is increased, a constricted seaway oasis therefore becomes much more favorable as the Snowball ages. As with the channel oasis, we find that the constricted seaway oasis is significantly less likely in FOAM than the other models. This implies that considerations of oasis solutions in the past using FOAM output are likely to be conservative.

5. Conclusions

[32] The main conclusions of this work are as follows:

[33] 1. All tested GCMs produce a similar pattern of atmospheric circulation. This causes a precipitation minus evaporation pattern that is consistent across models, with net evaporation in the tropics, which confirms that sea glaciers should flow equatorward in a Snowball Earth.

[34] 2. The Hadley cell is much stronger in all GCMs than in the modern and increases with increasing CO_2 in all GCMs. This is important because of the thick clouds that significantly warm the Snowball form in the Hadley ascent region. The increase in Hadley circulation strength with increasing CO_2 is consistent with large increases in tropopause height.

[35] 3. Warmer GCMs export more heat from the tropics to higher latitudes, as do all GCMs individually as the CO_2 is increased. Heat export from the tropics is therefore a negative feedback on Snowball deglaciation.

[36] 4. We find that in the axisymmetric approximation, sea glacier flow is efficient enough to cause roughly uniform sea glacier thickness regardless of the temperature and strength of precipitation minus evaporation that a GCM produces. This thickness can be predicted from the GCM's mean surface temperature.

[37] 5. The axisymmetric sea glacier model produces a thin-ice Snowball solution when forced by output from all GCMs if the penetration depth of solar radiation into ice is large enough (and an albedo of 0.6 is used). Future research into whether a thin-ice Snowball solution is possible should therefore focus on ice properties, rather than meteorological forcing.

[38] 6. We find that both the channel and constricted seaway oases become more favorable as the CO_2 and temperature increase, implying that the time right after a Snowball Earth is entered is the most dangerous for the survival of photosynthetic marine life. This is due to the decrease in sea glacier thickness outside the oasis as the Snowball warms.

[39] **Acknowledgments.** We thank Brian Rose, Stephen Warren, and an anonymous reviewer for helpful comments. We thank Malte Jansen for helping us improve our discussion of the Snowball Hadley circulation. D.S.A. and D.D.B.K. acknowledge support from NSF DMS-0940261, which is part of the NSF Math Climate Research Network. D.S.A. acknowledges support from an Alfred P. Sloan Research Fellowship. We acknowledge the German Research Foundation (DFG) program for the initiation and intensification of international collaboration. R.T.P. was supported by NSF ATM-0933936. This work was partially supported by the Max Planck Society for the Advancement of Science. The ECHAM6 simulation was performed at the German Climate Computing Center (DKRZ) in Hamburg, Germany. The authors thank GENCI (Grand Equipement National de Calcul Intensif) and the CEA (Commissariat à l'Energie Atomique) for providing the computer power necessary for the LMDz simulation.

References

Abbot, D. S., and I. Halevy (2010), Dust aerosol important for Snowball Earth deglaciation, *J. Clim.*, *23*(15), 4121–4132, doi:10.1175/2010JCLI3378.1.

Abbot, D. S., and R. T. Pierrehumbert (2010), Mudball: Surface dust and Snowball Earth deglaciation, *J. Geophys. Res.*, *115*, D03104, doi:10.1029/2009JD012007.

Abbot, D. S., I. Eisenman, and R. T. Pierrehumbert (2010), The importance of ice vertical resolution for Snowball climate and deglaciation, *J. Clim.*, *23*(22), 6100–6109, doi:10.1175/2010JCLI3693.1.

Abbot, D. S., A. Voigt, and D. Koll (2011), The Jormungand global climate state and implications for Neoproterozoic glaciations, *J. Geophys. Res.*, *116*, D18103, doi:10.1029/2011JD015927.

Abbot, D. S., A. Voigt, M. Branson, R. T. Pierrehumbert, D. Pollard, G. Le Hir, and D. D. Koll (2012), Clouds and Snowball Earth deglaciation, *Geophys. Res. Lett.*, *39*, L20711, doi:10.1029/2012GL052861.

Alder, J. R., S. W. Hostetler, D. Pollard, and A. Schmittner (2011), Evaluation of a present-day climate simulation with a new coupled atmosphere-ocean model GENMOM, *Geosci. Model Dev.*, *4*(1), 69–83, doi:10.5194/gmd-4-69-2011.

Barnes, P., D. Tabor, and J. C. F. Walker (1971), The friction and creep of polycrystalline ice, *Proc. R. Soc. London A*, *324*(1557), 127–155.

Barreiro, M., A. Cherchi, and S. Masina (2011), Climate sensitivity to changes in ocean heat transport, *J. Clim.*, *24*(19), 5015–5030.

Campbell, A. J., E. D. Waddington, and S. G. Warren (2011), Refugium for surface life on Snowball Earth in a nearly-enclosed sea? A first simple model for sea-glacier invasion, *Geophys. Res. Lett.*, *38*, L19502, doi:10.1029/2011GL048846.

Chandler, M., and L. Sohl (2000), Climate forcings and the initiation of low-latitude ice sheets during the Neoproterozoic Varanger glacial interval, *J. Geophys. Res.*, *105*(D16), 20,737–20,756.

Collins, W. D., et al. (2004), Description of the NCAR Community Atmosphere Model (CAM 3.0), *NCAR Tech. Note, NCAR/TN–464+STR*, Natl. Cent. for Atmos. Res., Boulder, Colo., 214 pp.

Dima, I. M., and J. M. Wallace (2003), On the seasonality of the Hadley cell, *J. Atmos. Sci.*, *60*(12), 1522–1527.

Donnadieu, Y., F. Fluteau, G. Ramstein, C. Ritz, and J. Besse (2003), Is there a conflict between the Neoproterozoic glacial deposits and the Snowball Earth interpretation: An improved understanding with numerical modeling, *Earth Planet. Sci. Lett.*, *208*(1-2), 101–112.

Fang, M., and K. K. Tung (1996), A simple model of nonlinear Hadley circulation with an ITCZ: Analytic and numerical solutions, *J. Atmos. Sci.*, *53*, 1241–1261.

Goodman, J. C. (2006), Through thick and thin: Marine and meteoric ice in a "Snowball Earth" climate, *Geophys. Res. Lett.*, *33*, L16701, doi:10.1029/2006GL026840.

Goodman, J. C., and R. T. Pierrehumbert (2003), Glacial flow of floating marine ice in "Snowball Earth", *J. Geophys. Res.*, *108*(C10), 3308, doi:10.1029/2002JC001471.

Held, I. M., and A. Y. Hou (1980), Nonlinear axially symmetric circulations in a nearly inviscid atmosphere, *J. Atmos. Sci.*, *37*(3), 515–533.

Herweijer, C., R. Seager, M. Winton, and A. Clement (2005), Why ocean heat transport warms the global mean climate , *Tellus, Ser. A*, *57*(4), 662–675.

Hoffman, P. F., and Z.-X. Li (2009), A palaeogeographic context for Neoproterozoic glaciation, *Palaeogeogr. Palaeoclimatol. Palaeoecol.*, *277*, 158–172.

Hoffman, P. F., and D. P. Schrag (2000), Snowball Earth, *Sci. Am.*, *282*(1), 68–75.

Hoffman, P. F., and D. P. Schrag (2002), The snowball Earth hypothesis: Testing the limits of global change, *Terra Nova*, *14*(3), 129–155.

Hoffman, P. F., A. J. Kaufman, G. P. Halverson, and D. P. Schrag (1998), A Neoproterozoic snowball Earth, *Science*, *281*(5381), 1342–1346.

Hourdin, F. et al. (2006), The LMDz4 general circulation model: Climate performance and sensitivity to parametrized physics with emphasis on tropical convection, *Clim. Dyn.*, *27*(7–8), 787–813, doi:10.1007/s00382-006-0158-0.

Hu, Y., J. Yang, F. Ding, and W. R. Peltier (2011), Model-dependence of the CO_2 threshold for melting the hard Snowball Earth, *Clim. Past*, *7*(1), 17–25, doi:10.5194/cp-7-17-2011.

Hyde, W. T., T. J. Crowley, S. K. Baum, and W. R. Peltier (2000), Neoproterozoic "Snowball Earth" simulations with a coupled climate/ice-sheet model, *Nature*, *405*(6785), 425–429.

Jacob, R. (1997), Low frequency variability in a simulated atmosphere ocean system, PhD thesis, Univ. of Wisconsin-Madison, Madison, Wis.

Khairoutdinov, M., C. DeMott, and D. Randall (2008), Evaluation of the simulated interannual and subseasonal variability in an AMIP-Style simulation using the CSU multiscale modeling framework, *J. Clim.*, *21*(3), 413–431, doi:10.1175/2007JCLI1630.1.

Khairoutdinov, M. F., and D. A. Randall (2001), A cloud resolving model as a cloud parameterization in the NCAR community climate system model: Preliminary results, *Geophys. Res. Lett.*, *28*(18), 3617–3620, doi:10.1029/2001GL013552.

Kirschvink, J. (1992), Late Proterozoic low-latitude global glaciation: The snowball Earth, in *The Proterozoic Biosphere: A Multidisciplinary Study*, edited by Schopf, J., and C. Klein, pp. 51–52, Cambridge Univ. Press, New York.

Le Hir, G., G. Ramstein, Y. Donnadieu, and R. T. Pierrehumbert (2007), Investigating plausible mechanisms to trigger a deglaciation from a hard snowball Earth, *C. R. Geosci.*, *339*(3–4), 274–287, doi:10.1016/j.crte.2006.09.002.

Le Hir, G., Y. Donnadieu, G. Krinner, and G. Ramstein (2010), Toward the snowball Earth deglaciation, *Clim. Dyn.*, *35*(2–3), 285–297, doi:10.1007/s00382-010-0748-8.

Li, D., and R. T. Pierrehumbert (2011), Sea glacier flow and dust transport on Snowball Earth, *Geophys. Res. Lett.*, *38*, L17501, doi:10.1029/2011GL048991.

Lindzen, R. S., and A. Y. Hou (1988), Hadley circulations for zonally averaged heating centered off the equator, *J. Atmos. Sci.*, *45*(17), 2416–2427.

Liu, Y., and W. R. Peltier (2010), A carbon cycle coupled climate model of Neoproterozoic glaciation: Influence of continental configuration on the formation of a "soft snowball", *J. Geophys. Res.*, *115*, D17111, doi:10.1029/2009JD013082.

McKay, C. (2000), Thickness of tropical ice and photosynthesis on a snowball Earth, *Geophys. Res. Lett.*, *27*(14), 2153–2156.

Micheels, A., and M. Montenari (2008), A snowball Earth versus a slushball Earth: Results from Neoproterozoic climate modeling sensitivity experiments, *Geosphere*, *4*(2), 401–410, doi:10.1130/GES00098.1.

O'Gorman, P. A., and T. Schneider (2008), The hydrological cycle over a wide range of climates simulated with an idealized GCM, *J. Clim.*, *21*, 3815–3832, doi:10.1175/2007JCLI2065.1.

Peltier, W. R., Y. G. Liu, and J. W. Crowley (2007), Snowball Earth prevention by dissolved organic carbon remineralization, *Nature*, *450*(7171), 813–818.

Pierrehumbert, R. T. (2004), High levels of atmospheric carbon dioxide necessary for the termination of global glaciation, *Nature*, *429*(6992), 646–649, doi:10.1038/nature02640.

Pierrehumbert, R. T. (2005), Climate dynamics of a hard snowball Earth, *J. Geophys. Res.*, *110*, D01111, doi:10.1029/2004JD005162.

Pierrehumbert, R. T., D. S. Abbot, A. Voigt, and D. Koll (2011), Climate of the Neoproterozoic, *Annu. Rev. Earth Planet. Sci.*, *39*, 417–460, doi:10.1146/annurev-earth-040809-152447.

Pollard, D., and J. F. Kasting (2005), Snowball Earth: A thin-ice solution with flowing sea glaciers, *J. Geophys. Res.*, *110*, C07010, doi:10.1029/2004JC002525.

Pollard, D., and J. F. Kasting (2006), Reply to comment by Stephen G. Warren and Richard E. Brandt on "Snowball Earth: A thin-ice solution with flowing sea glaciers", *J. Geophys. Res.*, *111*, C09017, doi:10.1029/2006JC003488.

Rose, B. E. J., and D. Ferreira (2013), Ocean heat transport and water vapor greenhouse in a warm equable climate: A new look at the low gradient paradox, *J. Clim.*, doi:10.1175/JCLI-D-11-00547.1, in press.

Schneider, T. (2006), The general circulation of the atmosphere, *Annu. Rev. Earth Planet. Sci.*, *34*(1), 655–688.

Schneider, T., and S. Bordoni (2008), Eddy-mediated regime transitions in the seasonal cycle of a Hadley circulation and implications for monsoon dynamics, *J. Atmos. Sci.*, *65*(3), 915–934.

Schneider, T., P. A. O'Gorman, and X. J. Levine (2010), Water vapor and the dynamics of climate changes, *Rev. Geophys.*, *48*, RG3001, doi:10.1029/2009RG000302.

Stevens, B., et al. (2013), The atmospheric component of the MPI-M earth system model: ECHAM6, *J. Adv. Model. Earth Syst.*, doi:10.1002/jame.20015, in press.

Stone, P. H. (1978), Constraints on dynamical transports of energy on a spherical planet, *Dyn. Atmos. Oceans*, *2*(2), 123–139.

Thompson, S. L., and D. Pollard (1997), Greenland and Antarctic mass balances for present and doubled atmospheric CO_2 from the GENESIS version-2 global climate model, *J. Clim.*, *10*(5), 871–900.

Thuburn, J., and G. C. Craig (1997), GCM tests of theories for the height of the tropopause, *J. Atmos. Sci.*, *54*, 869–882.

Tziperman, E., I. Halevy, D. T. Johnston, A. H. Knoll, and D. P. Schrag (2011), Biologically induced initiation of Neoproterozoic snowball-Earth events, *Proc. Natl. Acad. Sci. U. S. A.*, *108*(37), 15,091–15,096, doi:10.1073/pnas.1016361108.

Tziperman, E., D. S. Abbot, Y. Ashkenazy, H. Gildor, D. Pollard, C. G. Schoof, and D. P. Schrag (2012), Continental constriction and oceanic ice-cover thickness in a snowball-earth scenario, *J. Geophys. Res.*, *117*, C05016, doi:10.1029/2011JC007730.

Voigt, A., and D. S. Abbot (2012), Sea-ice dynamics strongly promote Snowball Earth initiation and destabilize tropical sea-ice margins, *Clim. Past*, *8*, 2079–2092, doi:10.5194/cp-8-2079-2012.

Voigt, A., and J. Marotzke (2010), The transition from the present-day climate to a modern Snowball Earth, *Clim. Dyn.*, *35*(5), 887–905, doi:10.1007/s00382-009-0633-5.

Voigt, A., D. S. Abbot, R. T. Pierrehumbert, and J. Marotzke (2011), Initiation of a Marinoan Snowball Earth in a state-of-the-art atmosphere-ocean general circulation model, *Clim. Past*, *7*, 249–263, doi:10.5194/cp-7-249-2011.

Voigt, A., I. M. Held, and J. Marotzke (2012), Hadley cell dynamics in a virtually dry Snowball Earth atmosphere, *J. Atmos. Sci.*, *69*, 116–128, doi:10.1175/JAS-D-11-083.1.

Walker, C., and T. Schneider (2005), Response of idealized Hadley circulations to seasonally varying heating, *Geophys. Res. Lett.*, *32*, L06813, doi:10.1029/2004GL022304.

Walker, C. C., and T. Schneider (2006), Eddy influences on Hadley circulations: Simulations with an idealized GCM, *J. Atmos. Sci.*, *63*(12), 3333–3350.

Warren, S. G., and R. E. Brandt (2006), Comment on "Snowball Earth: A thin-ice solution with flowing sea glaciers" by David Pollard and James F. Kasting, *J. Geophys. Res.*, *111*, C09016, doi:10.1029/2005JC003411.

Warren, S. G., R. E. Brandt, T. C. Grenfell, and C. P. Mckay (2002), Snowball Earth: Ice thickness on the tropical ocean, *J. Geophys. Res.*, *107*(C10), 3167, doi:10.1029/2001JC001123.

Wetherald, R. T., and S. Manabe (1975), The effects of changing the solar constant on the climate of a general circulation model, *J. Atmos. Sci.*, *32*(11), 2044–2059.

Winton, M. (2003), On the climatic impact of ocean circulation, *J. Clim.*, *16*(1), 2875–2889.

Yang, J., W. Peltier, and Y. Hu (2012a), The initiation of modern "soft Snowball" and "hard Snowball" climates in CCSM3. Part I: The influence of solar luminosity, CO_2 concentration and the sea-ice/snow albedo parameterization, *J. Clim.*, *25*, 2711–2736, doi:10.1175/JCLI-D-11-00189.1.

Yang, J., W. Peltier, and Y. Hu (2012b), The initiation of modern "soft Snowball" and "hard Snowball" climates in CCSM3. Part II: Climate dynamic feedbacks, *J. Clim.*, *25*, 2737–2754, doi:10.1175/JCLI-D-11-00190.1.

Yang, J., W. R. Peltier, and Y. Hu (2012c), The initiation of modern soft and hard Snowball Earth climates in CCSM4, *Clim. Past*, *8*, 907–918, doi:10.5194/cp-8-907-2012.